COMPARISONS OF KINEMATICAL RETRIEVALS WITHIN A SIMULATED SUPERCELL: DUAL-DOPPLER ANALYSIS VS. ENKF DATA ASSIMILATION

Corey K. Potvin[1], Louis Wicker[1] and Alan Shapiro[2]

[1]*NOAA National Severe Storms Laboratory, Norman, OK, USA, corey.potvin@noaa.gov*
[2]*School of Meteorology, and Center for Analysis and Prediction of Storms, Univ. of Oklahoma, Norman, OK, USA*
(Dated: 26 August 2011)

I. INTRODUCTION

One of the most valuable applications of dual-Doppler radar data is 3-D wind retrieval within convective storms. Since radars generally provide the only dense observations of storms above the ground, such retrievals are critical to illuminating storm kinematics and dynamics. Of course, proper interpretation of any analysis requires consideration of the analysis uncertainty. In addition, knowledge of the relative strengths and weaknesses of different radar-data analysis methods is required to design mobile radar deployment strategies and fixed radar networks that maximize the value of collected observations. Thorough understanding of the errors associated with different wind retrieval techniques is therefore critical to maximizing their use in advancing understanding of convective storms.

Dual-Doppler analysis (DDA) techniques provide a sophisticated way to retrieve the 3-D storm wind field from radar observations. However, substantial DDA errors can arise from a number of sources including finite observational resolution, incomplete radial velocity coverage due to earth curvature and precipitation-free regions, and rapid flow evolution during the analysis period. Assimilating dual-radar data using an ensemble Kalman filter (EnKF) ideally mitigates these errors by producing analyses consistent with both the radar observations and an NWP model. However, violations of the optimality conditions for the EnKF and errors in the NWP model and ensemble initialization inevitably limit improvements to the wind retrieval. It is therefore unclear under what conditions the EnKF should produce more accurate wind retrievals than DDA. Even more unclear is how the errors in single-radar EnKF wind analyses compare to typical DDA errors.

To examine this issue, we compare EnKF and DDA wind retrievals of a numerically-simulated supercell. The emulated radars observe the supercell at close range and use observational sampling characteristics typical of supercell-intercepting mobile radars. The forecast model used by the EnKF in the tests presented herein is identical to that used for the truth simulation except that it is run at coarser resolution. Given that significant errors in current NWP models arise from a number of sources, these experiments likely provide an overly optimistic estimate of the maximum value added by using the EnKF rather than DDA to retrieve supercell kinematics. A more realistic assessment will be provided by future EnKF experiments with a more imperfect model (e.g., perturbed microphysical parameterization scheme).

II. METHODS

The numerical supercell used in our experiments was generated using the National Severe Storms Laboratory Collaborative Model for Multiscale Atmospheric Simulation (NCOMMAS; Wicker and Skamarock 2002; Coniglio et al. 2006). The simulation proceeded on a stationary $102.4 \times 102.4 \times 20$ km domain with 200-m horizontal and vertical spacing. A fully dual-moment version of the Ziegler et al. (1985) microphysics scheme (Mansell et al. 2010) was used. The simulated supercell is qualitatively representative of atmospheric supercells.

As in Yussouf and Stensrud (2010), we increase the realism of the assimilated pseudo-observations by emulating the radar beam rather than generating point measurements, and by computing the pseudo-observations at the (spherical) radar gridpoints rather than at the model gridpoints. Pseudo-observations of reflectivity Z^{obs} and Doppler velocity V_r^{obs} are generated from the model Z, u, v, and w using the technique of Wood et al. (2009). This technique emulates the power-weighted averaging of radial velocities and reflectivities of scatterers within a Gaussian radar beam. Earth curvature and beam refraction, but not beam attenuation, are also emulated. Reflectivity observations < 0 dBZ are set to 0 dBZ to emulate the practice of treating missing or very low reflectivities (likely associated with non-meteorological scatterers) as "no-precipitation" observations to suppress spurious convection in the ensemble (Tong and Xue 2005). To emulate the lack of radial velocity data in regions of low signal-to-noise ratio, radial velocity observations are only computed in regions with $Z^{obs} > 5$ dBZ.

The emulated radars are located at the southern corners of the analysis domain indicated in Fig. 1. The radars sample every 150 m in range and 1.0° in azimuth and have half-power and effective beam widths of 0.89° and 1.39°, respectively. Each volume scan takes 3 min to complete and includes the following elevation angles (°): 0.5, 1.5, 2.5, 3.5, 4.5, 6.0, 7.5, 9.0, 10.5, 12.5, 14.5, 16.5, 19.0, 21.5, 24.0, 27.0, 30.0 and 33.0. To simulate observational non-simultaneity, the individual sweeps in each VCP are binned by elevation angle, and blocks of sweeps valid at higher elevation angles are computed from model fields valid at later simulation times. To reduce the

storage requirements and to speed up the radar pseudo-observation generation, each block of sweeps is computed from the model data at a single time. To emulate typical measurement errors, the Z^{obs} and V_r^{obs} are perturbed with errors drawn from zero-mean Gaussian distributions with standard deviations of 2 dBZ and 2 m/s, respectively.

The NCOMMAS EnKF data assimilation scheme is based on the ensemble square root filter of Whitaker and Hamill (2002). The EnKF settings used in our experiments are representative of recent storm-scale EnKF studies. The ensemble comprises 40 members. The covariance localization factor is calculated using the Gaspari and Cohn (1999) correlation function with covariance estimation cutoff radii of 6 km in the horizontal and 3 km in the vertical. The data assimilation domain has roughly the same dimensions as the truth simulation domain, and has 600 m grid spacing. The sounding input to each individual ensemble member is obtained by adding random ($\sigma = 2$ m s^{-1}) perturbations to u and v at the top and bottom of the sounding used in the truth simulation. Ellipsoidal thermal bubbles are inserted in each member at $t = 0$ to initiate storms. The bubbles are randomly positioned within a 40-km horizontal box roughly centered on the initiation location of the storm in the truth simulation. The ensemble members are integrated from $t = 0$ until data assimilation begins at $t = 30$ min. This duration of pre-assimilation integration is sufficient for developing physically realistic covariances associated with convective cells in the ensemble, and thus maximizing the utility of radar data early in the assimilation period (e.g., Snyder and Zhang 2003; Dowell et al. 2004).

The observations are assimilated every two minutes using a two-minute window centered on t. The assimilation proceeds for 42 min, during which the supercell translates eastward from north of the western radar to north-northwest of the eastern radar (Fig. 1). Observational error standard deviations of 2 m s^{-1} and 5 dBZ are assumed in the filter. In the two-radar experiments, reflectivity is only assimilated from one radar since reflectivity observations from the second radar would provide very little independent observational information. Prior to assimilation, the observations are thinned to a 2-km quasi-horizontal grid on each conical scan surface using Cressman interpolation with a 1-km cutoff radius. The interpolated observations are then spatially translated to account for storm motion (the estimation of which is described below).

Two methods are used to maintain ensemble spread consistent with the ensemble forecast error variance. During each analysis update, 2-K ellipsoidal bubbles are added to regions where the observed reflectivity exceeds the ensemble-mean reflectivity by at least 30 dBZ. Additionally, smoothed perturbations are added to several of the model fields wherever the observed reflectivity exceeds 20 dBZ (additive noise method; Dowell and Wicker 2009).

The dual-Doppler wind retrievals are performed using the 3D-VAR technique described in Shapiro et al. (2009) and Potvin et al. (2011). The technique weakly satisfies the radial wind observations, the anelastic mass conservation equation and a smoothness constraint, and exactly satisfies the impermeability condition at the ground. The dual-Doppler analyses proceed on a 40 × 40 × 6 km

domain with grid spacing equal to that of the data assimilation domain (600 m). Simple advection-correction of observations is used to account for wind field translation between the analysis and observational times. The translational velocity components U and V are assumed to be spatiotemporally constant and are estimated from visual inspection of the observed reflectivity field at several heights at successive times. The estimates $U = 10$ m s^{-1} and $V = 0$ m s^{-1} are obtained in this case.

For both the DDA and EnKF retrievals, root-mean-square errors (RMSE) in the analyzed wind components u^a, v^a and w^a are computed over the lowest 6 km of the dual-Doppler analysis domain. The RMSE are only computed over analysis points located within 750 m of an observation from each radar. The verification wind fields are obtained by first filtering the true wind fields to damp wavelengths too small to be resolved on the 600-m analysis grids (i.e., < 1.2 km), then spatially interpolating the (filtered) fields to the (Arakawa C) EnKF grid and the (unstaggered) DDA grid.
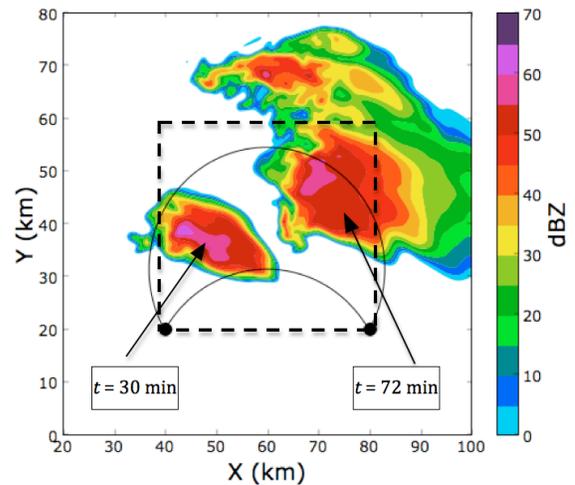
Fig. 1. Reflectivity at $z = 1$ km at $t = 30$ min and $t = 72$ min of the truth simulation. The black, dashed box represents the dual-Doppler domain. The 45° dual-Doppler lobe is also indicated.

III. INITIAL RESULTS

Potential detriments to the EnKF's ability to improve upon the DDA in our experiments include model errors, the "spin-up" time required for accurate ensemble covariances to develop, violations of the optimality conditions for the Kalman filter, potentially sub-optimal parameters and methods in our EnKF scheme, and sampling error due to the use of a finite ensemble. Sensitivity tests (not shown) suggest the latter two factors are not major sources of error in our experiments.

When data from both radars are assimilated, the RMSE in the EnKF-retrieved winds over the lowest 6 km are, overall, slightly lower than in the DDA winds (Fig. 2). This is an expected result of our using a model that is only mildly imperfect. When data are assimilated from only one radar, however, the errors increase substantially. Evidently, satisfying the NWP model does not sufficiently constrain the solution when only single-radar data are available. Given that real model errors are currently much larger than

those simulated in our experiments, these results suggest that use of the EnKF in retrieving supercell thunderstorm wind fields does not necessarily compensate for lack of dual-radar observations.
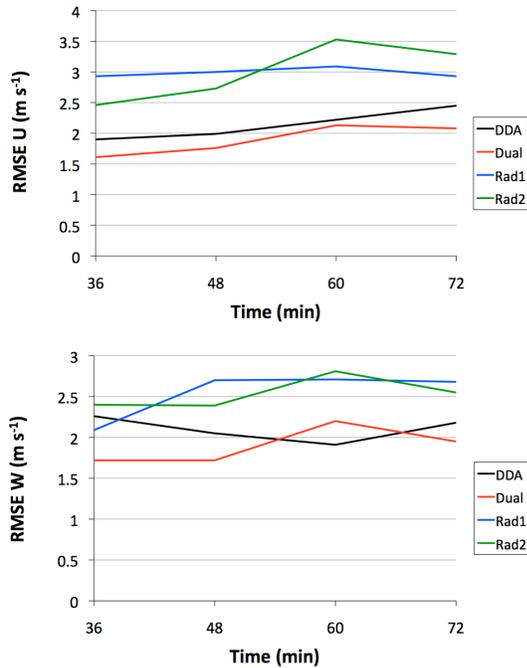
Fig. 2. RMSE u^a (top) and w^a (bottom) for DDA and EnKF wind retrievals.

IV. FUTURE WORK

The imperfect-model experiments presented above provide an optimistic view of typical NWP model errors, which arise from many sources other than coarse resolution. EnKF experiments with imperfect microphysics will be performed to further explore the impact of model error on the ability of the EnKF to improve upon wind retrievals obtained from DDA. The impact of radar cross-beam angle and scanning strategy will also be examined. Results of these new experiments will be presented at the conference.

VI. ACKNOWLEDGMENTS

VII. REFERENCES

Coniglio, M. C., D. J. Stensrud, and L. J. Wicker, 2006: Effects of upper-level shear on the structure and maintenance of strong quasi-linear mesoscale convective systems. *J. Atmos. Sci.*, **63**, 1231–1252.

Dowell, D. C., F. Zhang, L. J. Wicker, C. Snyder, and N. A. Crook, 2004: Wind and temperature retrievals in the 17 May 1981 Arcadia, Oklahoma, supercell: Ensemble Kalman filter experiments. *Mon. Wea. Rev.*, **132**, 1982–2005.

Dowell, D. C., and L. J. Wicker, 2009: Additive noise for storm-scale ensemble data assimilation. *J. Atmos. Oceanic Technol.*, **26**, 911–927.

Gaspari, G., and S. E. Cohn, 1999: Construction of correlation functions in two and three dimensions. *Quart. J. Roy. Meteor. Soc.*, **125,** 723–757.

Mansell, E. R., C. L. Ziegler, and E. C. Bruning, 2010: Simulated electrification of a small thunderstorm with two-moment bulk microphysics. *J. Atmos. Sci.*, **67**, 171–194.

Potvin, C. K., A. Shapiro, and M. Xue, 2011: Impact of a vertical vorticity constraint in variational dual-Doppler wind analysis: Tests with real and simulated supercell data. *J. Atmos. Oceanic Technol.*, accepted.

Shapiro, A., C. K. Potvin, and J. Gao, 2009: Use of a vertical vorticity equation in variational dual-Doppler wind analysis. *J. Atmos. Oceanic Technol.*, **26**, 2089–2106.

Snyder, C., and F. Zhang, 2003: Assimilation of simulated Doppler radar observations with an ensemble Kalman filter. *Mon. Wea. Rev.*, **131**, 1663–1677.

Tong, M., and M. Xue, 2005: Ensemble Kalman filter assimilation of Doppler radar data with a compressible nonhydrostatic model: OSS experiments. *Mon. Wea. Rev.*, **133**, 1789–1807.

Whitaker, J. S., and T. M. Hamill, 2002: Ensemble data assimilation without perturbed observations. *Mon. Wea. Rev.*, **130**, 1913–1924.

Wicker, L. J., and W. C. Skamarock, 2002: Time-splitting methods for elastic models using forward time schemes. *Mon. Wea. Rev.*, **130**, 2088–2097.

Wood, V. T., R. A. Brown, and D. C. Dowell, 2009: Simulated WSR-88D velocity and reflectivity signatures of numerically modeled tornadoes. *J. Atmos. Oceanic Technol.*, **26**, 876–893.

Yussouf, N., and D. J. Stensrud, 2010: Impact of phased-array radar observations over a short assimilation period: Observing system simulation experiments using an ensemble Kalman filter. *Mon. Wea. Rev.*, **138**, 517–538.

Ziegler, C. L., 1985: Retrieval of thermal and microphysical variables in observed convective storms. Part 1: Model development and preliminary testing. *J. Atmos. Sci.*, **42**, 1487–1509.